Acta Phys. Hung. B 26/1–2 (2006) 129–140
DOI: 10.1556/APH.26.2006.1–2.15

QUANTUM
ELECTRONICS

Trapping States of a Trapped Ion, Revisited

Peter E. Toschek[1] and Sascha Wallentowitz[2]

[1] Institut für Laser-Physik, Universität Hamburg, D-20355 Hamburg, Germany
Corresponding author; E-mail: toschek@physnet.uni-hamburg.de

[2] Facultad de Física, Pontificia Universidad Católica de Chile, Santiago, Chile

Received 31 July 2006

Abstract. The vibration of ions in the potential well of an ion trap has served for the first demonstration of laser cooling and is an essential ingredient of concepts for quantum information processing. The ion motion couples to a driven internal ion resonance such that the system obeys a Jaynes–Cummings (J–C) model that predicts coherently generated "trapping states" of the oscillatory excitation known from micro-maser dynamics. In the past, metastable states of the vibrational excitation of an individual trapped Ba ion had been observed. They were tentatively identified with the trapping states of the J–C model. Recently, an extension of this model including the spatial distribution of the light field has been shown to give rise to another type of trapping states that are robust under decoherence. The characteristics of these novel trapping states better represent the previously observed metastable vibronic states.

Keywords: trapped ion, vibration, trapping states
PACS: 32.80.Lg, 42.50.Vk

1. Introduction

Ions confined in various configurations of electrodynamic or electromagnetic traps and interacting with radiation are currently used as building blocks for quantum information processing (QIP) [1, 2]. Localized at local minima of the trapping potential, they are subjected to vibrations around these points of stability, and the vibrational modes are being used as carriers of information, in addition to the internal degrees of freedom [3, 4]. Ions in vibronic states may be selectively addressed by pulses of radiation that are resonant with a *vibrational sideband* of an electronic resonance of the ions [5,6]. A pulse whose time-integrated Rabi frequency — its dimensionless "area" — is well defined, discriminates vibronic states since the transition probability depends on the vibrational quantum number. Also, certain

1589-9535/ $ 20.00

manipulations require that a particular vibronic state is *inert* upon the interaction with the radiative pulse, or merely changes the sign of its wave function. In the past, such a condition had been implemented on an *electronic* resonance when shining, upon a gas of atoms, pulses of resonant radiation whose area is an integer multiple of 2π. This arrangement warrants the atoms, having undergone a full absorption–emission cycle, eventually to be left in their original ground state, provided that radiative loss is negligible during the cycle (Fig. 1). This kind of process is the basis of what is known as "self-induced transparency" of radiation (SIT) in the transmission of light pulses through a resonant absorber [7,8]. Even the light pulses have been shown to become stable: Back action by reemitted light does shape the transmitted pulses and allows deviations of both the input pulse shape and pulse area from their steady-state value. Partial dissipation forms each pulse to approach a train of stationary pulses whose total area equals a multiple of 2π: a particular type of "solitons".

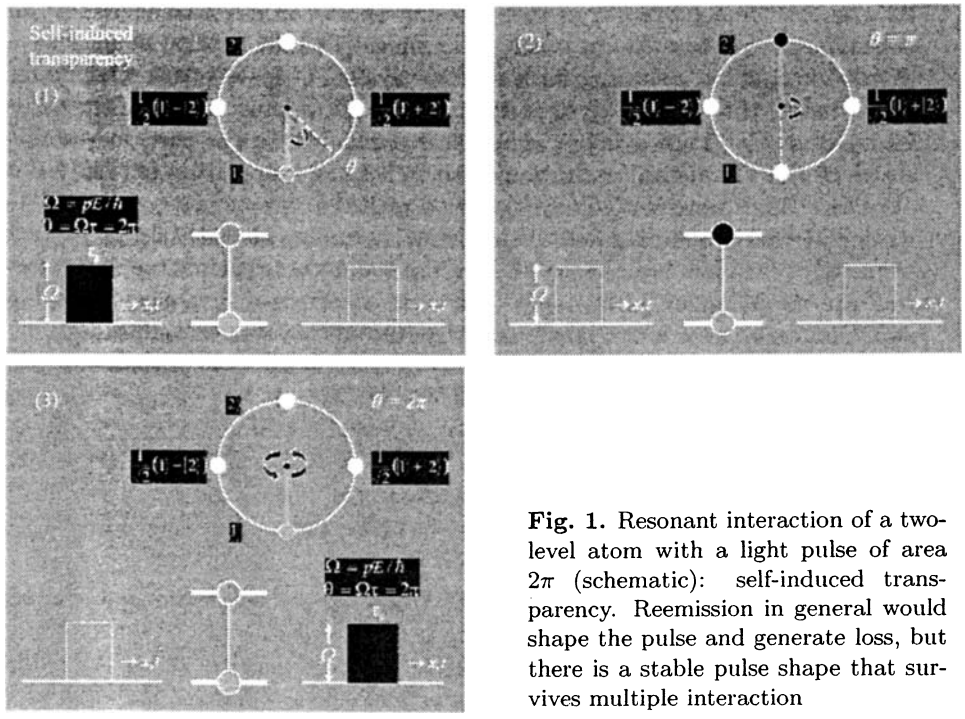

Fig. 1. Resonant interaction of a two-level atom with a light pulse of area 2π (schematic): self-induced transparency. Reemission in general would shape the pulse and generate loss, but there is a stable pulse shape that survives multiple interaction

The interaction of a field mode of radiation — representing an oscillator — with a "two-level" atom equivalent to a spin is described in terms of the Jaynes–Cummings model (J–C) [9]. In particular, J–C has been operative upon modelling the dynamics of a micro-maser field [10, 11]. Here, special excitation numbers of

the field mode in a microwave resonator have been predicted and later observed [12] that resist the further growth of that maser field upon increased pumping by a beam of inverted atoms. These "trapping states" of the field represent states of dynamic metastability of the coupled system made up of "spin" and field.

2. Vibrational Trapping States

It has been noticed some time ago that the vibrational dynamics of a two-level atom that moves in a potential well and also represents an oscillator — a mechanical one — coupled to a "spin", is likewise governed by J–C. Thus, vibrational trapping states have been expected to show up upon *vibronic sideband* excitation to an electronic resonance of such atoms, e.g. ions in a trap [13–16]. From a solution of J–C, the probabilities of excitation and survival of such an atom in state n upon resonant sideband excitation are

$$w(n+1\,|\,n) = \sin^2\left(\sqrt{n+1}\,\theta_s/2\right) \tag{1}$$

and

$$w(n\,|\,n) = \cos^2\left(\sqrt{n+1}\,\theta_s/2\right)\,, \tag{2}$$

respectively, where $\theta_s = |\Omega_s|\tau_s$, and $\Omega_s = i\eta\Omega$ is the Rabi frequency on the first-order red-shifted sideband in the Lamb–Dicke limit, $\eta \ll 1$ [17]. This limit requires the spatial extension of the atom's vibronic vacuum wave function not to exceed the wavelength of the radiation. Thus, the trapping condition reads

$$\theta_s\sqrt{n_0+1} = 2\pi m \tag{3}$$

for any trapping state n_0, and m integer.

In a series of experiments on a single barium ion, localised in an electrodynamic (Paul) trap, laser light at 492 nm, being slightly down-tuned from resonance, excited

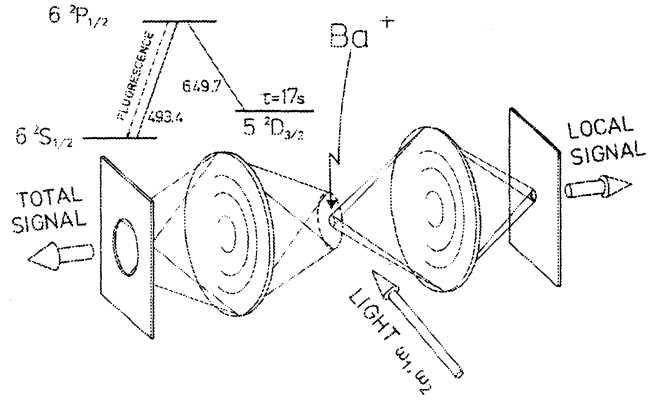

Fig. 2. Binary detection of resonance fluorescence from a single barium ion, excited by blue (493 nm) and red (650 nm) laser light

the ion's $S_{1/2}$–$P_{1/2}$ line, and the resonance scattering was detected [18]. In order to counteract optical pumping into the $^2D_{3/2}$ state, irradiation by laser light at 650 nm, resonant with the $^2D_{3/2}$–$^2P_{1/2}$ line, repumped the ion from its $D_{3/2}$ level into its ground state. The ion's laser-excited resonance scattering was recorded via two channels (Fig. 2). In the first one, the scattered light was focussed onto a pinhole of 35 μm diameter before being detected as the "local" signal. This signal showed its full extent only when the ion was "cold", i.e. pointlike, and distributed over its lowest vibronic levels; upon higher vibrational excitation, the signal was cut down. In the other channel, a corresponding diaphragm was some 200 μm wide, such that the full signal was detected even when the ion was vibrationally excited and the image of its orbit had grown to substantial size. This signal served for the discrimination of light fluctuations. Then, the ratio of the two signals represented a measure of the extension of the vibrational orbit of the ion. An example of the temporal

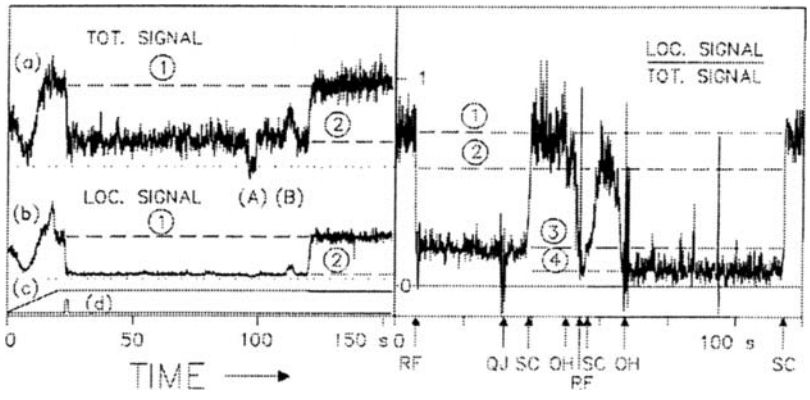

Fig. 3. Left: Total signal (a), local signal (b) vs. time, pitch of red laser (c), and power of irradiated radio frequency resonant with secular motion of ion (d). Signal level 1 corresponds to optimum cooling the ion, levels 2, ..., 4 to metastable vibronic states (I_b = 12 W/cm^2, I_r = 25 W/cm^2). Right: Local signal normalized by total signal, vs. time. Various perturbations (RF: pulsed rf heating, QJ: quantum jump, OH: incremental variation of red-laser tuning, SC: spontaneous onset of laser cooling) take the ion to various metastable orbits (I_b = 12 W/cm^2, I_r = 20 W/cm^2) (from Ref. [18])

variation of this ratio is shown in Fig. 3. Instantaneous perturbations either took place spontaneously (for instance, by off-resonant electronic Raman excitation of the dark state $^2D_{5/2}$, causing a break in the light scattering and laser cooling), or they were applied intentionally (pulsed rf heating, or incremental detuning of the red repump laser). The recording of the normalized local signal while perturbations took place resulted in four reproducible signal levels, the highest of which was attributed to the optimally cooled state of the ion, whereas the other three signal levels were considered metastable vibrational states. The latter ones have been

tentatively attributed to SIT-like trapping states, according to Eq. (3). A rough estimate of the quantum numbers corresponding to the metastable levels, however, showed them to somewhat exceed the lowest expected trapping numbers.

Although this experiment involved continuous light, the ion had to alternate between the $S_{1/2}$ ground state and the $D_{3/2}$ metastable level in a stochastic sequence of excitations and deexcitations. A sequence of regular cycles can be achieved when pump-laser pulses are made alternating with pulses that drive the dipole-forbidden resonance to the $D_{3/2}$ metastable level. In what follows it is shown that a cold ion in a trap, subjected to alternated pumping and vibronic-sideband driving, not only gives rise to metastable vibronic states of SIT type. In addition, there is another type of "trapping states" that result from the *spatial structure* of the light field.

3. Dynamics of a Laser-Pumped and Laser-Driven Ion in the Trapping Potential

The ion is described as a three-level atom with ground state $|1\rangle$ and an excited state $|2\rangle$, typically of same parity as $|1\rangle$ (Fig. 4). Pumping the ion to this state $|2\rangle$ via a resonance level $|3\rangle$ is considered to alternate with the ion's return to the ground state $|1\rangle$, driven on a vibrational sideband. The system is modelled by the equation of motion of the vibronic density operator [19]

$$\dot{\hat{\rho}} = -\frac{i}{\hbar}\left[\hat{H}_0 + \hat{H}_r(t), \hat{\rho}\right] + \text{relaxation terms}\,, \tag{4}$$

$$\hat{H}_0 = \hbar\nu\hat{a}^\dagger\hat{a} = \sum_{i=l}^{3}\hbar\omega\hat{A}_{ii}\,, \tag{5}$$

where $r = p$, s for the intervals of pumping and sideband driving, respectively,

$$\hat{H}_p = \frac{1}{2}\hbar\Omega_p\hat{A}_{31}e^{-i\omega_p t} + \text{h.c.}\,, \tag{6}$$

$$\hat{H}_s = \frac{1}{2}\hbar\Omega\hat{A}_{21}e^{i(k\hat{x}-\omega t)} + \text{h.c.}\,, \tag{7}$$

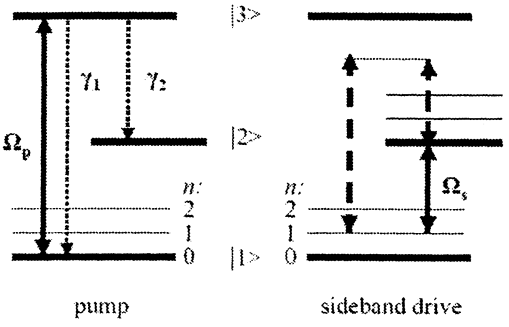

Fig. 4. Preparation of a trapping state: Intervals of pumping the ion, by laser light (Rabi frequency Ω_p), to level $|2\rangle$ alternate with intervals of laser-driving the first vibrational sideband of line 1-2 directly (Rabi frequency Ω_s), or Raman-like (dashed arrows)

$\hat{A}_{ij} = |i\rangle\langle j|$ generates transitions between the electronic states i and j, $\hat{x} = (a^\dagger + a)\eta c/\omega$, and $\hat{a}$ and $\hat{a}^\dagger$ are the annihilation and creation operators of a vibrational quantum, respectively. The relaxation terms include photonic recoil on the centre-of-mass motion of the ion. With the pumping interval being long enough, a stationary state is approached, when the population is accumulated in level 2. The corresponding matrix element $\hat{\rho}_{22} = \langle 2|\hat{\rho}|2\rangle$ still operates on the vibrational degree of freedom in the subsequent radiative driving, e.g. on the first red-shifted sideband, $\omega = \omega_{21} - \nu$. This driving induces transitions between the vibronic states $|2, n\rangle$ and $|1, n+1\rangle$, where n labels the ion's vibronic eigenstates in the potential well of the trap. In the interaction picture, and with the rotating-wave approximation in the vibration frequency, the drive Hamiltonian turns into

$$\hat{H}_s = \frac{1}{2}\hbar\Omega_s \hat{A}_{21}\hat{f}(\hat{n};\eta)\hat{a} + \text{h.c.}\,, \tag{8}$$

where $\Omega_s = i\eta\Omega$ is the Rabi frequency on the first-order red-shifted sideband in the Lamb–Dicke limit [19]. The (normally ordered) operator function

$$\hat{f}(\hat{n};\eta) = (\eta\sqrt{\hat{n}})^{-1} J_1(2\eta\sqrt{\hat{n}})\, e^{-\eta^2/2} \tag{9}$$

of the number operator $\hat{n} = a^\dagger a$ takes care of spatially more extended vibronic states that may violate the Lamb–Dicke condition, and J_1 is the first-order Bessel function.

4. Coherent Generation of Trapping States

The temporal evolution of the system during the kth driving interval is modelled by a time-evolution operator acting on the vibronic density operator [19]. The expectation values of the occupation density of the vibronic states are shown to obey a recurrence relation whose coefficients represent the probabilities for vibrational excitation, or survival, in one pump-drive cycle. It turns out that in Eqs. (1) and (2), the argument $\Omega_s\sqrt{n+1}$ must be replaced by

$$\Omega_s^{n,n+1} = \Omega_s \langle n+1|e^{-ik\hat{x}}|n\rangle = \Omega_s f(n;\eta)\sqrt{n+1} = \frac{\Omega_s}{\sqrt{n+1}} L_n^{(1)}(\eta^2)\, e^{-\eta^2/2} \tag{10}$$

such that the probabilities of excitation and survival become

$$w_{\text{coh}}(n+1|n) = \sin^2\left(\Omega_s^{n,n+1}\tau_s/2\right)\,, \tag{11}$$

$$w_{\text{coh}}(n|n) = \cos^2\left(\Omega_s^{n,n+1}\tau_s/2\right)\,, \tag{12}$$

respectively, and $L_n^{(1)}$ is an associated Laguerre polynomial. Thus, there exist two *independent* types of trapping conditions for a particular vibronic state n to become a trapping state n_0:

$$\Omega_s\tau_s f(n_0;\eta)\sqrt{n_0+1} = 2\pi m\,, \tag{13}$$

(m integer) that is of SIT type, modified only by the factor $f(n_0;\eta)$. This trapping requires coherent interaction of light and atomic polarisation. In addition, further vibrational excitation also discontinues when

$$f(n_0;\eta) = 0 \tag{14}$$

holds. This condition is associated with the zeroes of the Laguerre polynomial in (10). It results from a Franck–Condon-type overlap integral of neighbouring vibronic eigenstates.

In order to make a particular eigenstate a trapping state, it may be addressed by properly choosing the driving pulse area $\theta_s = \Omega_s \tau_s$ according to the SIT condition (13). Alternatively, one may pick an arbitrary, so far non-trapping value of θ_s and select an effective Lamb–Dicke parameter η that matches condition (14). Setting η may be achieved when two laser beams drive the ion in a Raman-like configuration: the angle subtended by the beams determines the effective Lamb–Dicke parameter.

Transition probabilities for vibrational sideband excitation according to trapping conditions (13) or (14) being matched, and with $n_0 = 50$, are shown in Fig. 5. Note that the probability values below the trapping state, derived from Eq. (14) and shown in plot (b), exceed the corresponding values in plot (a). Thus, although the ion's continued excitation slows down close to n_0 anyway, this approach will be faster with the Franck–Condon type of trapping. Moreover, whereas SIT trapping requires coherent dynamics, the F–C type is supposed to show up even in the presence of decoherence.

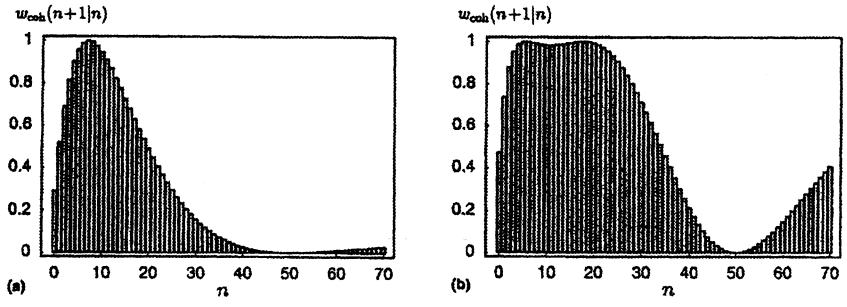

Fig. 5. Coherent transition rates $w_{\mathrm{coh}}(n+1\,|\,n)$ for (a) $\eta = 0.1$, $|\Omega_s|\tau_s = 1.149$ [trapping state condition (13) for $n_0 = 50$], and for (b) $\eta = 0.268$ [trapping state condition (14) or $n_0 = 50$], and $|\Omega_s|\tau_s = \pi/2$ (from Ref. [19])

5. Incoherent Generation of Trapping States

The above approaches to the generation of trapping states require any kind of dephasing to be negligible, e.g. the effects of phase fluctuations of the driving lasers, spontaneous emission of the ion, and collisions with background gas atoms. This requirement poses a substantial challenge in any experiment. Fortunately, in contrast

with SIT trapping, the dynamics of Franck–Condon trapping turns out *independent of the coherence* of the interactions. Thus, the actual demonstration of this trapping scheme seems far easier, and the involved states are supposed more robust than with an approach sensitive to decoherence.

The rate constant of dephasing, γ, may depend on the vibrational quantum number n for certain relaxation processes [20–22]. Here we neglect such a complication, and also the radiative recoil exchanged in the ion–light interactions. The latter effect is included, however, in the numerical calculations whose results are shown below.

The system is still assumed to obey the condition of resolved sidebands such that we have now $\Omega_s < \gamma < \nu$. Solution of the master equation (4) under this condition results in the recurrence relation [19]

$$P_n(t_{k+1}) = w_{\mathrm{inc}}(n \mid n-1)\, P_{n-1}(t_k) + w_{\mathrm{inc}}(n \mid n)\, P_n(t_k) \tag{15}$$

for the distribution over the vibrational states

$$P_n(t_k) = \langle n \mid \hat{\rho}_{11} + \hat{\rho}_{22} \mid n \rangle\,, \tag{16}$$

which is similar to the recurrence relation upon decoherence lacking. However, the probabilities for excitation and survival are now

$$w_{\mathrm{inc}}(n+1 \mid n) = \frac{1}{2} - \frac{1}{2}\exp\left[-\gamma_n(\eta)\tau_s\right] \tag{17}$$

and

$$w_{\mathrm{inc}}(n \mid n) = \frac{1}{2} + \frac{1}{2}\exp\left[-\gamma_n(\eta)\tau_s\right]\,, \tag{18}$$

respectively. The effective damping coefficients

$$\gamma_n(\eta) = \frac{4\,|\Omega_s|^2}{\gamma}\,(n+1)\,f^2(n;\eta) \tag{19}$$

now depend on the vibrational quantum number non-linearly in general, but linearly in the Lamb–Dicke limit ($f \to 1$). The trapping condition

$$w(n+1 \mid n) = 0\,, \quad \text{if} \quad n = n_0 \tag{20}$$

requires

$$\gamma_n(\eta) \propto \left[L_n^{(1)}(\eta^2)\right]^2 = 0\,, \tag{21}$$

and this relation shows the trapping states being determined *by the zeroes of the Laguerre polynomial.* From the recurrence relation (15), the vibrational distribution emerges as a sum of binomial distributions

$$P_n(t_k) = \sum_{l=0}^{n} \binom{k}{n-l} 2^{-k}\, P_l(t_0)\,, \tag{22}$$

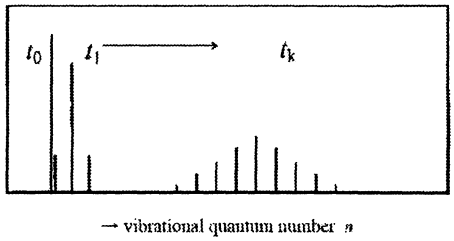

Fig. 6. A vibronic vacuum state at t_0 evolves into a distribution of three components after the first pump-drive cycle (t_1), and into a binomial distribution of more components after k cycles (t_k)

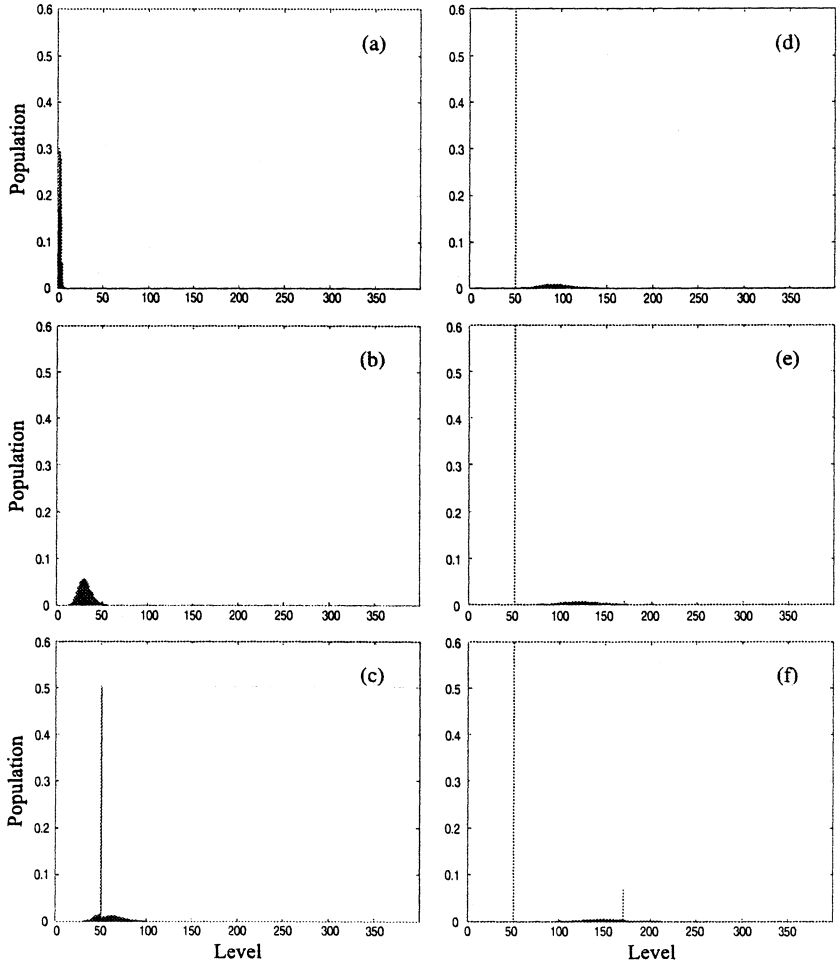

Fig. 7. Temporal evolution of the vibronic vacuum state at increasing number k of pump-probe cycles (a–f: k = 5, 60, 120, 180, 240, 300). The trapping state $n_0 = 50$ accumulates 60 percent of the occupation. Light recoil, included in the numerical calculations, generates spillover that accumulates in higher trapping states

each of which derives from a particular component of the initial distribution and is characterised by a mean value $l + k/2$ and variance $k/4$ (Fig. 6). After many iteration cycles, i.e. after long time, the variance of the total distribution

$$\langle [\Delta n(t)]^2 \rangle / \langle n(t) \rangle \to \frac{1}{2} \tag{23}$$

approaches 1/2, and this sub-Poissonian level signals amplitude squeezing. Close to a trapping state n_0, the limiting variance even approaches zero, as it is compatible with a vibronic number state.

The evolution of an ion initially in its vibronic vacuum state is shown in Figs. 7a–f. Notice the spill-over beyond the first trapping state $n_0 = 50$, most of which accumulates in the next trapping state. This phenomenon results from imperfections of the trapping introduced by including, in the computation, the radiative recoil on the absorbing or emitting ion. Further calculations using various amplitude values of the sideband-driving light have shown the system to develop into an almost pure number state upon higher saturation.

In Fig. 8, the evolution of the variance of the vibrational distribution is shown for three intensities of the sideband driving light, parameterized as $4|\Omega_s|^2 \tau/\gamma$. The variance remains non-zero, for the same kind of imperfections, caused by the radiative recoil.

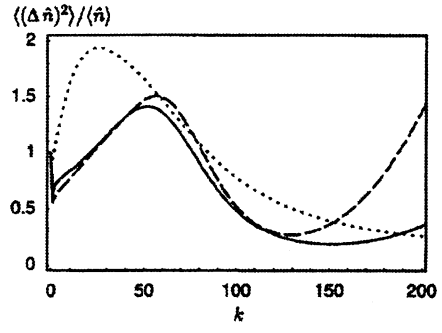

Fig. 8. Variance vs. number of cycles, k, for incoherent trapping $n_0 = 50$, $\eta = 0.268$. Spontaneous recoil included. Saturation parameter $2\Omega_s^2 \tau_s/\gamma = 0.2$ (dotted), 1.0 (solid), 2.0 (dashed) (from Ref. [19])

6. Summary

A quantum system characterised by an internal resonance, or "spin" resonance, coupled to a harmonic oscillator shows a fundamental peculiarity: Continued excitation of the oscillator degree of freedom via sidebands to the spin resonance does not smoothly continue to arbitrarily high values of excitation, but stops at certain "trapping states" of the oscillator. This phenomenon has been analysed for an example of potential application in QIP, namely an ion vibrating in the potential well of an ion trap. It is well known [17] that the excitation probability periodically varies with the quantum number of the vibrational excitation. The probability vanishes when the system, driven on a particular sideband — say, the first red-shifted

one, $|2, n_0\rangle \rightarrow |1, n_0 + 1\rangle$ — undergoes an integer number of Rabi cycles in configuration space, during the time of interaction with the light. Light pulses propagating in a resonant gas have been shown to lock to such cycles and yield the phenomenon of "self-induced" transparency.

On top of this, there is an alternative mechanism for making vanish the excitation probability at certain vibrationally excited states, when the spatial structure of light field is taken into account. Now, the emergence of trapping states derives from the interference of overlapping vibrational wave functions, as in molecular Franck–Condon factors. This novel mechanism has been shown insensitive against decoherence, drastically relieving the preconditions for demonstration in a real system. During the iterative excitation of the ionic motion, say, from the vacuum state, a binomial distribution over vibronic states emerges that is amplitude-squeezed and approaches a number state, when the ion's vibrational excitation comes close to trapping. Former observations of metastable vibronic states of single barium ions in a miniature Paul trap are now attributed to having demonstrated this incoherent mechanism.

Acknowledgments

This research was supported by grants FONDECYT No. 1051072 and Milenio ICM No. P02-049F.

References

1. D.P. DiVincenzo, *Fortschr. Phys.* **48** (2000) 771.
2. A.M. Steane and D.M. Lucas, *Fortschr. Phys.* **48** (2000) 839.
3. J.I. Cirac and P. Zoller, *Phys. Rev. Lett.* **74** (1995) 4091.
4. C. Monroe, D. Leibfried, B.E. King, D.M. Meekhof, W.M.Itano and D.J. Wineland, *Phys. Rev.* **A55** (1997) R2489.
5. B. Appasamy, Y. Stalgies and P.E. Toschek, *Phys. Rev. Lett.* **80** (1998) 2805.
6. B.E. King, C.S. Wood, C.J. Myatt, Q.A. Turchette, D. Leibfried, W.M. Itano, C. Monroe and D.J. Wineland, *Phys. Rev. Lett.* **81** (1998) 1525.
7. W. Krieger and P.E. Toschek, *Phys. Rev.* **A11** (1975) 276.
8. W. Krieger, G. Gaida and P.E. Toschek, *Z. Physik* **B25** (1976) 297.
9. E.T. Jaynes and F.W. Cummings, *Proc. IEEE* **51** (1963) 89.
10. P. Filipowicz, J. Javanainen and P. Meystre, *Phys.Rev.* **A34** (1986) 3077.
11. R.J. Brecha, A. Peters, C. Wagner and H. Walther, *Phys.Rev.* **A46** (1992) 567.
12. M. Weidinger, B.T.H. Varcoe, R. Heerlein and H. Walther, *Phys. Rev. Lett.* **82** (1999) 3795.
13. Th. Sauter, H. Gilhaus, I. Siemers, R. Blatt, W. Neuhauser and P.E. Toschek, *Z. Phys.* **D10** (1988) 153.
14. C.A. Blockley, D.F. Walls and H. Risken, *Europhys. Lett.* **17** (1992) 509.

15. R. Blatt, J.I. Cirac and P. Zoller, *Phys. Rev.* **A52** (1995) 518.
16. S. Wallentowitz, W. Vogel, I. Siemers and P.E. Toschek, *Phys. Rev.* **A54** (1996) 943.
17. P. Meystre and M. Sargent III, *Elements of Quantum Optics*, Springer, Berlin, 1990.
18. Th. Sauter, H. Gilhaus, W. Neuhauser, R. Blatt and P.E. Toschek, *Europhys. Lett.* **7** (1988) 317.
19. S. Wallentowitz, W. Vogel and P.E. Toschek, *Opt. Commun.* **239** (2004) 109.
20. S. Schneider and G.J. Milburn, *Phys. Rev.* **A57** (1998) 3748.
21. C. Di Fidio, S. Wallentowitz, Z. Kis and W. Vogel, *Phys. Rev.* **A60** (1999) R3393.
22. C. Di Fidio and W. Vogel, *Phys. Rev.* **A62** (2000) 031802(R).